Date: 2022-01-31 17:41 UTC

All sources 39 | Internet sources 38 | Plagiarism Prevention Pool 1

[0] www.researchsquare.com/article/rs-310002/latest.pdf
3.0% 41 matches
1 documents with identical matches

[2] www.researchgate.net/publication/324521864_NTilt_as_an_improved_enhanced_tilt_derivative_filter_for_edge_detection_of_potential_field_anomali
0.9% 22 matches

[3] www.sciencedirect.com/science/article/pii/S1464343X19300640
1.0% 26 matches

[4] www.researchgate.net/publication/351798389_Subsurface_structural_mapping_from_high-resolution_gravity_data_using_advanced_processing_meth
0.4% 23 matches

[5] www.mdpi.com/2075-163X/11/11/1247/htm
0.6% 11 matches

[6] www.sciencedirect.com/science/article/pii/S1464343X21003198
0.3% 17 matches
1 documents with identical matches

[8] link.springer.com/article/10.1007/s13201-020-01224-0
0.0% 14 matches

[9] www.researchgate.net/publication/322465584_Interpretation_of_Aeromagnetic_Data_to_Delineate_Structural_Complexity_Zones_and_Porphyry_Intr
0.0% 12 matches

[10] www.sciencedirect.com/science/article/pii/S101836472100149X
0.4% 11 matches

[11] www.researchgate.net/publication/320228914_Application_of_directional_derivative_method_to_determine_boundary_of_magnetic_sources_by_total_
0.0% 9 matches

[12] www.sciencedirect.com/science/article/pii/S1464343X20303502
0.3% 10 matches

[13] www.researchgate.net/publication/328180053_Directional_tilt_derivatives_to_enhance_structural_trends_in_aeromagnetic_grids
0.3% 10 matches

[14] www.noveltyjournals.com/upload/paper/Interpretation of Aeromagnetic Data to-1248.pdf
0.0% 8 matches

[15] www.researchgate.net/figure/Total-Magnetic-Intensity-Map-of-the-study-area-showing-major-towns-flown-over_fig3_258389562
0.0% 9 matches

[16] link.springer.com/article/10.1007/s12665-021-10060-7
0.0% 8 matches

[17] www.researchgate.net/figure/Second-vertical-derivative-SV-anomaly-map-generated-from-EIGEN6C4-free-air-gravity-data_fig3_305749320
0.0% 9 matches

[18] link.springer.com/article/10.1007/s12517-021-06511-x
0.3% 4 matches

[19] www.researchgate.net/publication/306930503_Inferring_the_subsurface_basement_depth_and_the_structural_trends_as_deduced_from_aeromagnetic
0.0% 5 matches

[20] www.ijries.org/administrator/components/com_jresearch/files/publications/IJRIES_73_Final.pdf
0.0% 6 matches

[21] link.springer.com/article/10.1007/s42452-021-04263-7
0.2% 3 matches

[22] www.researchgate.net/profile/Ikechukwu-Ibeneme/publication/327115535_Improved_Mapping_of_the_Structural_Disposition_of_Some_Younger_Gr
0.0% 3 matches

[23] www.researchgate.net/publication/258820881_More_reliable_responses_for_time_integration_analyses
0.0% 2 matches

[24] www.researchgate.net/figure/Map-of-the-modulus-of-total-horizontal-gradient-THG-of-Bouguer-gravity-anomalous-field_fig3_236351777
0.0% 2 matches

[25] from a PlagScan document dated 2019-01-31 09:34
0.0% 2 matches

☑ [26] www.researchgate.net/figure/Location-of-the-Mamfe-sedimentary-basin-in-the-SW-region-of-Cameroon-and-SE-region-of_fig4_274068119
0.0% 3 matches

☑ [27] www.researchgate.net/figure/Improved-normalized-horizontal-tilt-angle-INH-map-of-the-Bouguer-anomaly-The-dashed_fig6_288836345
0.0% 2 matches

☑ [28] www.researchgate.net/figure/Geological-map-of-the-Federal-Capital-Territory-Abuja-showing-the-different-rock-types_fig2_320877631
0.0% 1 matches

☑ [29] link.springer.com/article/10.1007/s11053-020-09689-1
0.0% 1 matches

☑ [30] www.sciencedirect.com/science/article/pii/S0960077919304266
0.0% 1 matches

☑ [31] www.researchgate.net/figure/a-TMI-map-of-the-study-area-b-Reduced-to-the-pole-data-in-a-c-TDR-TDX-of-the-data-in-b_fig9_342424054
0.0% 1 matches

☑ [32] library.seg.org/doi/abs/10.1190/SEGJ2018-058.1
0.0% 1 matches

☑ [33] core.ac.uk/download/pdf/72842556.pdf
0.0% 1 matches

☑ [34] www.researchgate.net/figure/Synthetic-model-parameters-used-for-generating-the-synthetic-data_tbl1_316434713
0.0% 1 matches

☑ [35] link.springer.com/article/10.1007/s12517-021-07370-2
0.0% 1 matches

☑ [36] link.springer.com/article/10.1007/s11053-020-09725-0
0.0% 1 matches

☑ [37] www.researchgate.net/publication/317606884_Lineaments_and_tectonics_of_the_Sao_Pedro_and_Botucatu_ridge_region_-_Southeastern_Brazil
0.0% 1 matches

☑ [38] researchgate.net/figure/Synthetic-model-parameters-and-inversion-results_tbl1_318396419
0.0% 1 matches

☑ [39] onlinelibrary.wiley.com/doi/abs/10.1002/gj.3350220629
0.0% 1 matches

☑ [40] www.researchgate.net/figure/Location-and-geology-map-of-study-area-modified-from-12_fig7_268445649
0.0% 1 matches

15 pages, 3006 words

PlagLevel: 5.2% selected / 14.4% overall

87 matches from 41 sources, of which 40 are online sources.

Settings

Data policy: *Compare with web sources, Check against the Plagiarism Prevention Pool*

Sensitivity: *High*

Bibliography: *Bibliography excluded*

Citation detection: *Highlighting only*

Whitelist: --

Application of the enhanced edge detection filter in the exploratory mapping of geologic structures involving magnetic data in Southeast Nigeria

Abstract

Enhanced lineament detector and depth estimator involving modern aero-magnetic data were employed to study parts of the Obudu-Plateau and Lower-Benue-Trough with the aim of mapping thermo-tectonic geologic structures and estimating sediment thicknesses. In this investigation, the enhanced horizontal-gradient amplitude (EHGA) (applied to both simulated and actual data) and tilt depth approaches were operated. The simulated magnetic model employing the EHGA detector generated sharp and properly defined edges of magnetic bodies with the capacity to place peaks over source borders. The tilt-depth technique showed thin and thick sedimentations that vary from ~500 to ~1000 m and ~1500 to ~2500 m, respectively. The observed geologic structures trend mainly in the NW and NE, as well as minor N-S directions. These structures, generated by the Younger-Mesozoic-Granitic intrusions of calc-alkaline ring complexes, and the Santonian-Abakaliki Anticlinorium serve as paths for super enriched hydrothermal fluids migration and deposition. The applied methods can be used to decipher the geologic structures in alike zones around the world.

Keywords: Magnetic Method; EHGA; TDM; Lower Benue Trough; Obudu Plateau; Southeast Nigeria

1. Introduction

Geophysical studies involving the potential field (PF) techniques detect the small variations in physical rock properties (density and magnetization) (Telford 1990). These physical properties can offer information on the Earth's crustal structure (Melouah et al., 2021; Eldosouky et al., 2021a; Saada et al., 2021a, 2021b, 2022; Sehsah and Eldosouky, 2022; Ekwok et al., 2021a), basement framework (Ekwok et al., 2021b) as well as sediment thickness (Ekwok et al., 2021a).

The magnetic method is a remarkably powerful tool for mapping geologic structures (Eldosouky et al., 2022; Ekwok et al., 2022a, 2022b; Eldosouky and Saada, 2020) including regional geologic boundaries (Ekwok et al., 2019). These characteristic features make magnetic data an essential component of mineral assessment programs (Eldosouky and Elkhateeb, 2018). Furthermore, magnetic data can be effectively applied in hydrocarbon exploration, unexploded ordnance detection, archaeological studies, etc. (Saada et al., 2022; Essa and Elhussein, 2018; Telford, 1990).[3]

Generally, the procedures of magnetic data reductions, enhancements, display, and interpretation have advanced considerably over the years (Essa and Elhussein, 2018). Edge enhancement techniques are commonly used to highlight geologic structures caused by magnetic variations (Pham et al., 2021a). A lot of these advanced methodologies are available in many works of literature (e.g., Eldosouky and Mohamed, 2021; Pham et al., 2021a, 2021b). Edge detection filters like the analytic signal (Roest et al., 1992), horizontal-gradient amplitude (Cordell et al., 1985), theta (Wijns et al.[2], 2005), tilt-angle filter (Miller and Singh, 1994), normalized-horizontal derivative (Cooper and Cowan, 2006), tilt-angle of the horizontal-gradient amplitude (Ferreira et al., 2013), etc., have been used by various researchers in their separate studies. Pham et al. (2021a) reported the fairly hazy limitations associated with these methods. To address these limitations, and effectively map geologic structures including subtle lineaments, advanced processing methods like the improved normalized-horizontal tilt-angle (Li et al., 2014), improved theta method (Yuan et al., 2016), enhanced tilt angle (Nasuti et al., 2019), total directional-theta method and enhanced-horizontal derivative amplitude (Zareie and Moghadam, 2019), were developed. The findings of this investigation which is expected to improve our experience of the pattern and distribution of geologic structures, involved aero-magnetic data and improved edge detectors like the tilt -angle of the horizontal-gradient amplitude (THGA), enhanced-horizontal-gradient amplitude (EHGA) involving 3D models, and Tilt depth method

(TDM). The efficacy of the EHGA filter was tested using synthetic data and the results compare very favourably with synthetic data. In general, defining geologic structures in combination with hydrothermally altered rocks is necessary for mineral explorations (Ekwok et al., 2022a).

Previous magnetic studies in this region involved filtering methods like first- and second-vertical derivatives, total-horizontal and tilt-angle derivatives, downward continuation, source-edge-detection, and centre for exploration targeting (CET) including textural analysis and circular feature transform plug-ins (Ekwok et al., 2022a, 2020a, 2019). Mineralization is often connected with structural control and hydrothermal alteration caused by igneous intrusions (Dill et al., 2010). Tectonic processes generated faults, fractures, fissures, and dike swarms in the Cretaceous strata of the Obudu-Plateau (OP) and Lower-Benue-Trough (LBT) (Ekwok et al., 2021c). Tectonic events influence the localization, intensity, and characteristics of hydrothermal deposits, moreover the tendency and character of groundwater moves (Ekwok et al., 2020b). Outlining the geologic structures and hydrothermal-altered rocks is critical for mineral exploration (Sehsah et al., 2019).

2. The study area

2.1. Location

The area includes portions of the Cretaceous-Lower-Benue-Trough (CLBT) and the Precambrian-Obudu-Plateau (POP). It is located within the southeastern Nigerian states of Enugu, Ebonyi, and Cross River. the area lies between longitudes 7°30'E and 9°00'E and latitudes

6°00'N and 6°30'N. Figure 1 shows the topography (elevation) of the study area.

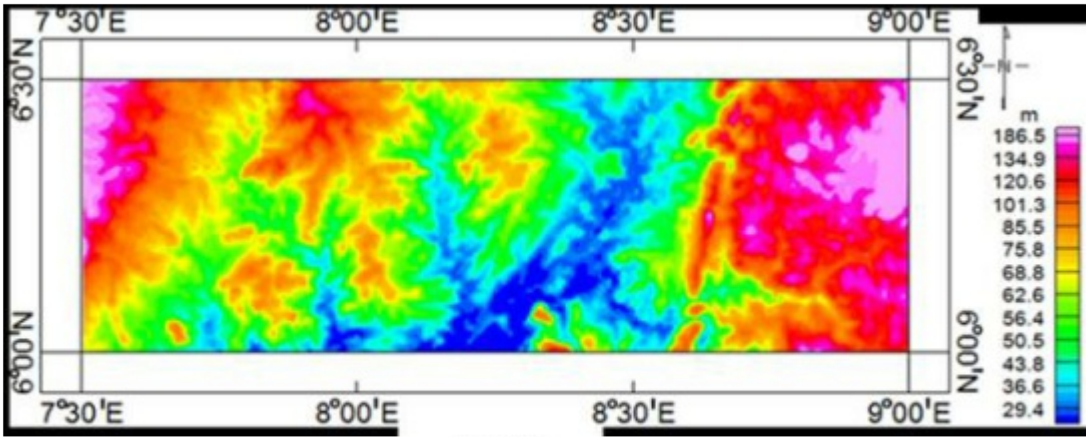

Fig. 1: Elevation (Topography) map of the investigated area.

2.2. The Geology

According to geologic age, the investigated region is placed in two of Nigeria's three geologic provinces, namely the POP and CLBT (Fig. 2).

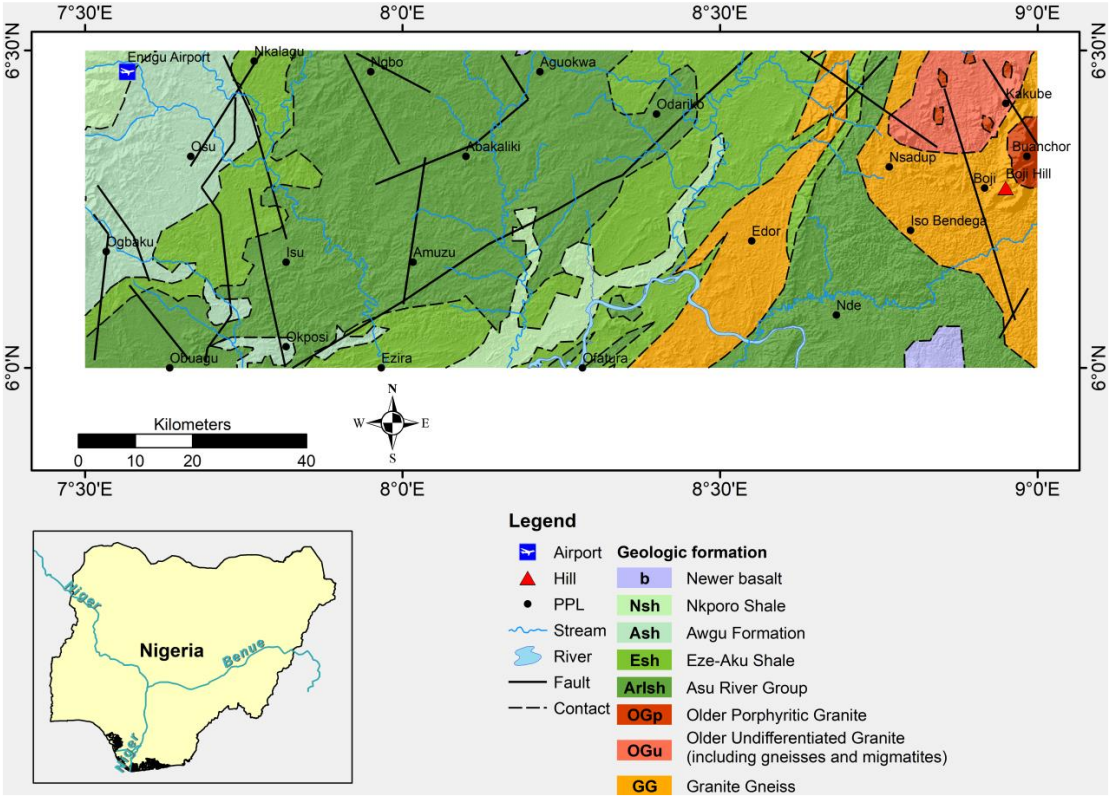

Fig. 2: Geologic map of the study region.

2.2.1. Precambrian Obudu Plateau (POP)

The Nigerian-Basement Complex (NBC) is assumed to have formed through time as a result of a sequence of tectono-thermal processes, with at least three phases of deformation described by Rahaman and Lancelot (1984). The lithologic groups in the basement complex include the migmatite-gneiss complex, schist belts, and older granites sets. The Migmatite-gneisses are regarded to be the earliest rocks in the NBC (Haruna, 2017). A substantial component of the complex is assumed to represent altered earlier crust, possibly from the Liberian period, that has been further affected by later-orogenies such as the Eburnean (2000+200 Ma) and Pan-African (600+150 Ma) orogenies, with the inclusion of the schist and granitoid belts (Haruna, 2017). Despite indications of sedimentation and distortion in Kibaran (1300-1100 Ma), no magmatic event of this period has been documented. The Kibaran was chaperoned by dates ranging from 900 to 450 Ma, indicating a Pan-African event that generated gneisses, migmatite, earlier granite intrusions, and other lithologic features (Haruna, 2017; Haruna and Mamman, 2005).

The POP which is an extension of the Bamenda-Massif is one of the Nigerian-Basement outcrops in southeast Nigeria (Agbi and Ekwueme, 2018). High-grade metamorphic rocks make up the lithological differences in the area (Agbi and Ekwueme, 2018; Ukwang et al., 2012).

2.2.2. Cretaceous-Lower-Benue-Trough (CLBT)

The tectonic evolution of the continental basins to the south of Nigeria, as well as other basins in the West- and Central-African-Rift systems, can be traced back to the poly-fragmentation phase of the Gondwana supercontinent into current South-American and African Plates (Late Jurassic to Early Cretaceous) (Bumby and Guiraud, 2005; Wilson and Guiraud, 1992). This

disintegration occurred before other key events like the continents migrating apart and the opening of the South-Atlantic (Cratchley et al., 1984; Burke et al., 1972).

The LBT is a segment of Nigeria's Benue Trough, a northeast-southwest trending linear basin. The area is covered with a thick layer of Cretaceous sedimentary successions that were deposited in rapidly shifting settings. Sedimentation began in the basin after a sequence of transgressive-regressive stages (Kogbe, 1981). The Ebonyi and Abakaliki formations make up the oldest and most basic Asu River Group (ARG). Shale, limestone, clay, and siltstone, sandstone come in various thicknesses (Cenomanian in age) (Kogbe, 1981). Eze-Aku (Turonian) Formation (EAF), which overlies the ARG, is overlooked by limestone, sandstone, and shales. The Nkporo/Enugu (dark-blue) Formation is part of a pro-deltaic habitat that becomes increasingly restricted higher in the Mamu Formation. Basal coal seams are covered by interchanging strata of sandstone and fine-grained shales as some Nsukka Formation coal seams (Doucet and Popoff, 1985).

3. Methods

3.1. Enhanced horizontal gradient amplitude

In this investigation, a cutting-edge filter was proposed (Pham et al., 2020c) centred on the EHGA and the horizontal-gradient derivatives of magnetic grids to define the lateral boundaries of geologic lineaments. The EHGA operator can be given as:

$$EHGA = R\left(asin\left(p\left(\frac{\frac{\partial THG}{\partial z}}{\sqrt{\left(\frac{\partial THG}{\partial x}\right)^2+\left(\frac{\partial THG}{\partial y}\right)^2+\left(\frac{\partial THG}{\partial z}\right)^2}}-1\right)+1\right)\right), \quad (1)$$

where, p is a constant greater or equal to 2 (Pham et al., 2020c), $\frac{\partial THG}{\partial x}$, $\frac{\partial THG}{\partial y}$, and $\frac{\partial THG}{\partial z}$ are the derivatives in x, y, and z directions of the total-horizontal gradient (THG) (Cordell, 1979) that is approximated by:

$$THG = \sqrt{\left(\frac{\partial F}{\partial x}\right)^2 + \left(\frac{\partial F}{\partial y}\right)^2} \quad (2)$$

where $\frac{\partial F}{\partial x}$ and $\frac{\partial F}{\partial y}$ are the field derivative in x, y, and z directions, respectively, and k is a positive real number that is chose by the interpreter. In this research, k = 3 was employed to generate a simulated magnetic model to evaluate the sharpness of the EHGA filter. The model (Fig. 3a) which is characterised by 3D view consist of three prismatic bodies, whose parameters are obtainable in Table 1.

Table 1: Synthetic model parameters.

Parameters/Model label	A	B	C	D	E
x-coordinates of centre (km)	100	100	40	100	160
y-coordinates of centre (km)	65	55	28	28	28
Width (km)	3	3	30	30	30
Length (km)	150	150	30	30	30
Depth of top (km)	2	3	2	5	8
Depth of bottom (km)	5	6	5	8	11
Declination (°)	0	0	0	0	0
Inclination (°)	90	90	90	90	90
Magnetization (A/m)	1	-1.2	2.5	-2.5	2.5

The approximated magnetic anomaly relating to the model is shown in Fig. 3b. Fig. 3c shows the EHGA of data. It was witnessed that the EHGA technique can generate well defined edges for magnetic sources A, B, and C. It is observed that the peaks of the EHGA are located directly over the source borders, and this filter generates more reliable responses.

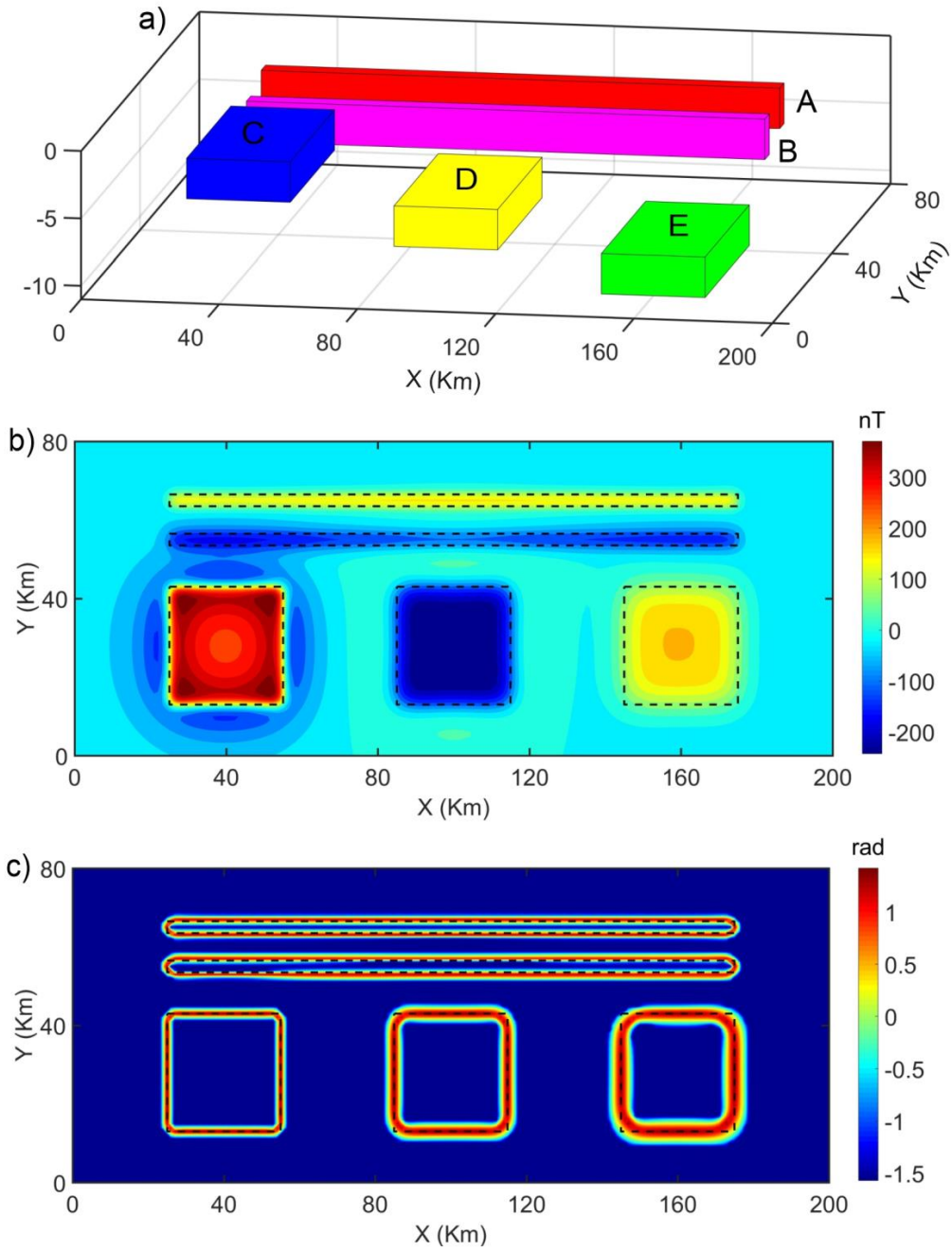

Fig. 3: (a) Three-dimensional view of the model, (b) its magnetic anomaly, and (c) the EHGA of the model.

3.2. Tilt depth method

A frequently employed enhancement technique for the potential field (PF) data f is the tilt-angle (T) (Miller and Singh 1994), which equates the amplitude of the vertical-derivative of the field utilizing its horizontal derivatives.

$$T = tan^{-1}\left|\frac{\frac{\partial f}{\partial z}}{\sqrt{\left(\frac{\partial f}{\partial x}\right)^2 + \left(\frac{\partial f}{\partial y}\right)^2}}\right| \quad (3)$$

Salem et al. (2007) elucidated that when the mathematical formulations for the vertical and horizontal gradients of the magnetic field over a vertical contact were entered into equation (3), they are simplified to:[2]

$$TDM = tan^{-1}\left(\frac{\Delta x}{\Delta z}\right) \quad (4)$$

where Δz and Δx are the vertical and horizontal distances from the prevailing approximation point to the centre of the top of the boundary. The TDM (Salem et al., 2007) suggested approximating the distance within the ±45° values of T, which was twice the depth Δz.

4. Results

The airborne-magnetic data were gathered by Fugro-Airborne-Surveys, Canada under the control of Nigerian-Geological-Survey-Agency (NGSA) (2005: 2010 in three phases (Adetona and Abu, 2013). The total aero-magnetic intensity (TAMI) map of the investigated region (Fig. 4) shows magnetic variations from - 905.790 nT to 210.626 nT. The Central (E-W) part is characterized by low intensity, while the southern, northeastern, and northern parts are of high intensity (Fig. 4).

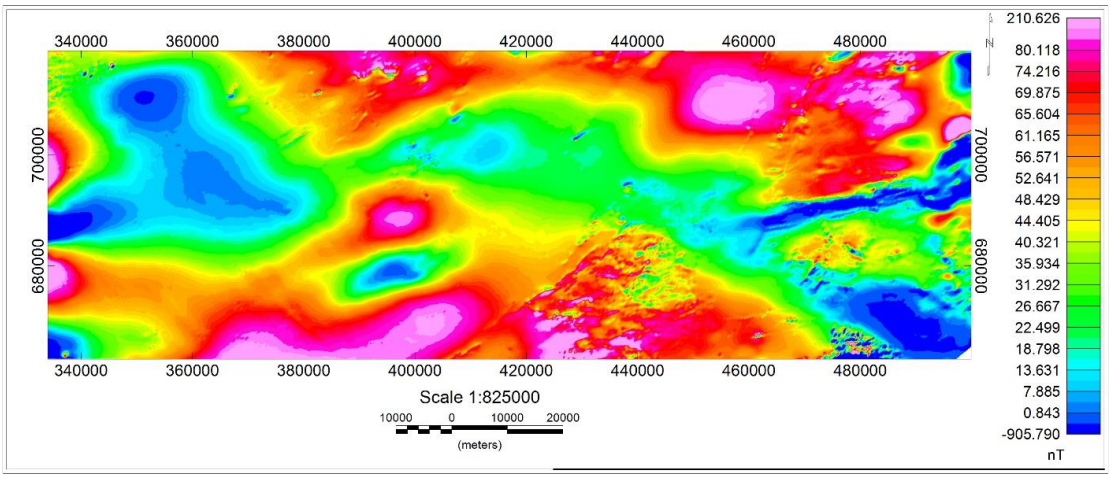

Fig. 4: The total aero-magnetic intensity data of the studied area.

[21]

The EHGA filter is applied to the TAMI data (aeromagnetic) of the study area (Fig. 5). The EHGA clearly outlines and refines the lineaments of the studies region.

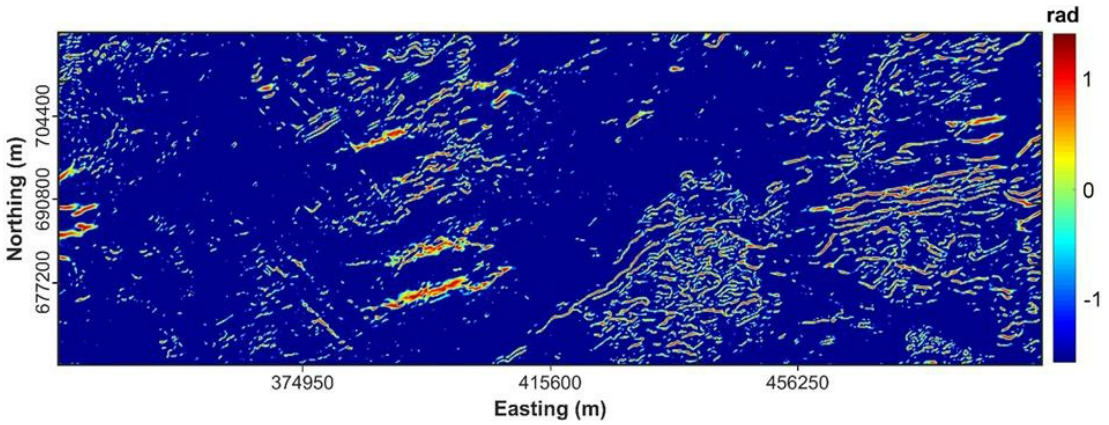

Fig. 5: The EHGA map of the studied region.

Figure 5 shows that the eastern part is highly-deformed than the western one.[2] The NE, ENE, and E-W directions are dominant to the east of the area while the ENE and NW are dominant to the west.

The depth-estimation technique involving TDM (Fig. 6) was employed to quantitatively define the consistencies of sediments in the study area. This method, like source parameter imaging, is

an enhanced technique for delineating the lateral positions and depths of magnetic sources (Ekwok et al., 2021a). This procedure is suitable for mapping single and multiple magnetic bodies with various shapes like isolated poles, dyke (prism), dipole, lines of poles, vertical contact, and susceptibility difference (Telford et al., 1990).

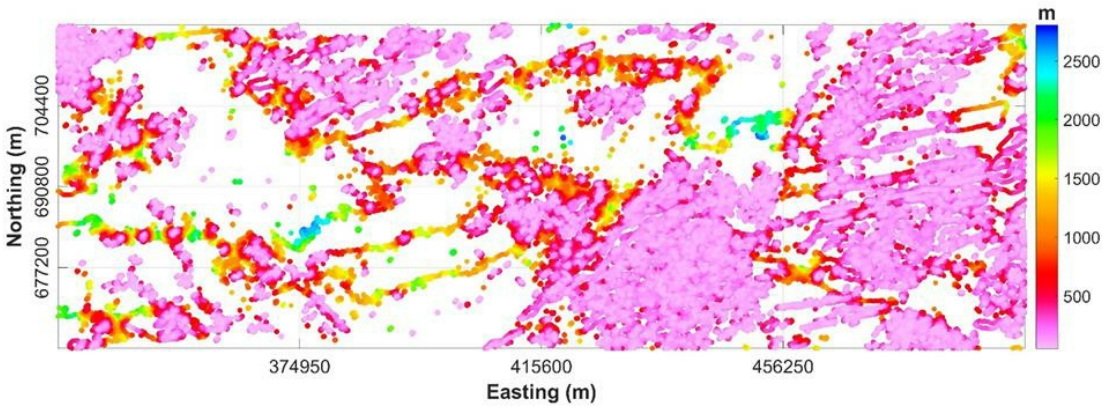

Fig. 6: Tilt-depth method map of the studied region.

Figure 6 shows TDM characterized by wide-ranging colours of blue-pink indicating various depth values. The depth range from ~1500 to ~2500 m as indicated by lemon green to blue reflects deep magnetic bodies while ~500 to ~1000 m (pink-yellow) shows the depth to shallow magnetic bodies. The maximum depth solution acquired employing TDM is ~2500 m and lies within the depth range documented in the region by former workers (Ekwok et al., 2022a, 2021a; Ofoegbu and Onuoha, 1991; Agagu and Adighije, 1983). Generally, the relatively thin sedimentation observed in the examined region is due to the post-depositional intrusions related to Abakaliki (Santonian) Anticlinorium (Ekwok et al., 2022a, 2022b, 2020a; Benkhelil, 1987) and exposed basements (Agbi and Ekwueme, 2018; Ukwang et al., 2012) in the eastern- and western-flanks, respectively.

5. Discussion

The EHGA detector of the structures proposed by Pham et al. (2020c) was employed to simulate the magnetic model with the object of examining the sharpness of the EHGA filter. Prismatic

bodies with characteristic parameters (Table 1) estimated the magnetic anomaly linked to the model (Fig 3). The projected magnetic anomaly related to the model is shown in Fig. 3b. The improved EHGA which sets peaks over source borders created well-defined and clear edges for sources A, B, and C (Fig. 3a). This detector has been reported to be a cutting-edge detector with better resolution than previous filters (Pham et al.,2022, 2021a, 2020c).

To image the linear structures, the EHGA lineaments were statistically analysed using a rose diagram (Fig. 7). Figures 5 and 7 which indicate the structural features such as faults and fractures etc., revealed high lineament density in the Precambrian basement area (eastern flank) triggered by the younger granitic intrusions of Mesozoic calc-alkaline ring complexes (Woakes et al., 1987). Also, the intermediate-low lineament density delineated in the western- and central-flanks of the investigated area are caused by the Abakaliki Santonian) Anticlinorium-related igneous intrusions (Benkhelil, 1987). These geologic structures, found in the underlying basement complex rocks and the overlying sedimentary layer, have major NW, ENE, and NE structural orientations, as well as minor N-S directions. These faults, fractures, etc., serve as conduits for super enriched hydrothermal fluids movement and deposition (Ekwok et al., 2022a, Mineral-Resources of the Western US, 2017; USGS, 2013; Dill et al., 2010). Similarly, geologic structures reveal porous and permeable zones which somewhat denote the groundwater potential of an area (Ekwok et al., 2020b; Murasingh and Jha, 2013).

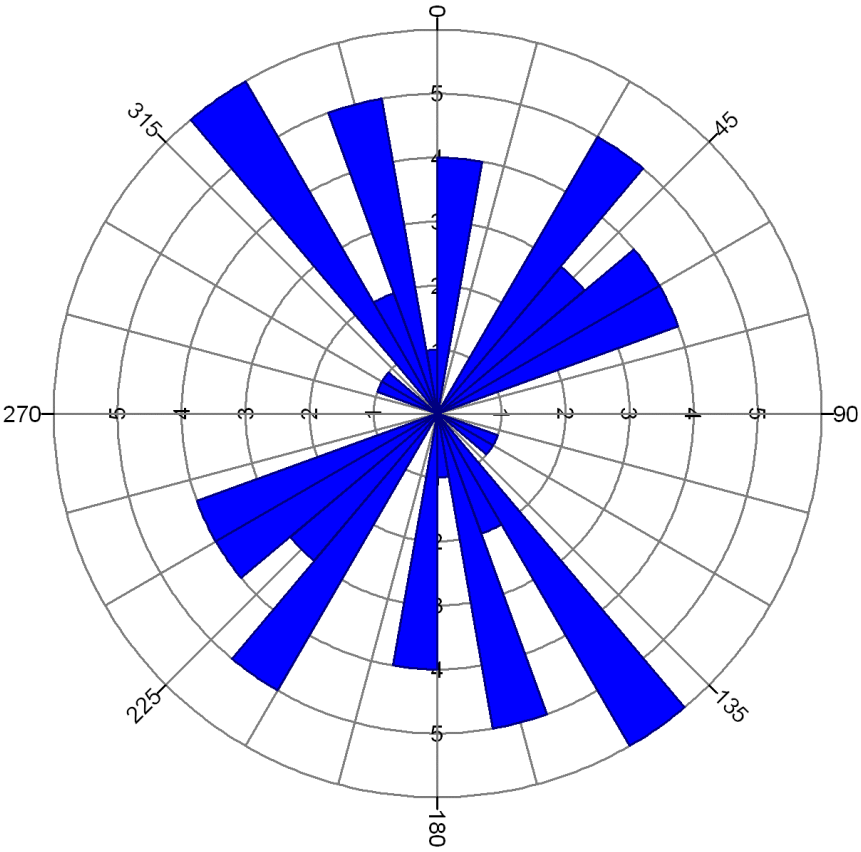

Fig. 7: Satellite lineament rose diagram of the studied region.

The TDM (Salem et al., 2007) is an enhanced depth determination method that generated a maximum depth value of about 2500 m. Studies involving magnetic datasets, Euler-Deconvolution (ED), and Source-Parameter-Imaging (SPI) depth estimation methods generated depth of ~2440.0 and ~2570.2 m respectively (Ekwok et al., 2022a, 2022b). Also, gravity investigation from ED and SPI revealed a maximum depth of ~2496.8 m and 2461.1m (Ekwok et al., 2022a) respectively. However, 2-D GM-SYS results showed a depth value of ~2922.0 m (Ekwok et al., 2022a). In our investigation, the estimated depth result from TDM verified the efficacy of depth values obtained by previous researchers. Furthermore, the thin sedimentary pile witnessed in the region is caused by the widespread occurrence of post-depositional Santonian

intrusions in this region of the LBT (Ekwok et al., 2019, 2020a; Akpan et al.[0], 2014), and extensive outcrops of the basement in the OP (Agbi and Ekwueme, 2018; Ukwang et al., 2012). Magnetic data involving enhanced filters that can be employed to outline geologic structures have been carried out by recent scholars (Pham et al., 2021c, 2020c; Pham, 2020a, 2020b). Delineation of fractures, faults, fissures, etc., using improved edge detector filters is for the polymetallic-magmatic-hydrothermal deposits explorations. Such study in the CLBT and the adjoining area is for hydrothermal modifications caused by tectonic events and their related base metal, massive sulphide, shear hosted gold, and some other deposits (Ekwok et al., 2022a, 2022b; Mineral-Resources of the Western US, 2017; USGS, 2013; Dill et al., 2013; Dill et al., 2010). The EHGA map (Fig. 5) indicated high lineament density in the POP that is caused by tectono-thermal activity that initiated the intrusions of Younger-Mesozoic-Granite of calc-alkaline Ring Complexes in the basement (Woakes et al., 1987). Likewise, the central and western regions are dominated by intermediate-low lineament density produced by Abakaliki (Santonian) Anticlinorium-related igneous intrusions (Benkhelil, 1987). Figures 5 and 7 show major NW and NE structural orientations, in addition to minor N-S trends.[5] The NE orientation of the structures coincides with the direction of the Nigerian BT (Benkhelil, 1987; Cratchley et al., 1984; Burke et al., 1972). Some major geologic structures are thought to have extended into the upper mantle (Ekwok et al., 2022a; Haruna, 2017). Several reports show that geologic structures serve as the pathway for migration and deposition of minerals (Elkhateeb et al., 2021; Mineral-Resources of the Western US, 2017; Elkhateeb and Eldosouky, 2016; USGS, 2013; Murasingh and Jha, 2013; Dill et al., 2010). The Igneous related-base metals (Akande and Muecke, 1993; Olade and Morton, 1985; Nwachukwu, 1972) and brine fields (Ekwok et al., 2022b; Tijani, 2004; Uma, 1998) in the CLBT, as well as the metallogenic minerals in the POP (Ekwok et al., 2022a; Haruna, 2017), are believed to be deposited in these structures.

6. Conclusion

Structural studies and depth estimation in some parts of the OP and LBT were carried out involving recent airborne-magnetic data, enhanced lineament detector, and depth estimator. Improved filtering filters (EHGA involving 3D models, real data, and Tilt depth solutions) were applied in this research. The computer-generated magnetic model employing EHGA detector positions peaks over source boundaries and produced sharp and well-defined boundaries for magnetic sources. The TDM which is an advanced depth estimation method revealed thin and thick sedimentations that vary from ~500 to ~1000 m and ~1500 to ~2500 m, respectively. This maximum depth value correlates strongly with recent studies involving other enhanced depth determination methods and high-resolution potential field data. The geologic structures that serve as channels for super-enriched hydrothermal fluids movement and deposition were mapped and observed to have major NW, ENE, and NE structural orientations with minor N-S directions. These structures that are abundant at the Basement-Precambrian area are regarded to be generated by the YoungerMesozoic-Granitic intrusions of calc-alkaline Ring-Complexes, and the Abakaliki Santonian) Anticlinorium.